Compression of laser pulses due to Raman amplification of plasma noises

A. A. Balakin ⬤, D. S. Levin, and S. A. Skobelev

Institute of Applied Physics of the Russian Academy of Sciences, 603950 Nizhniy Novgorod, Russia

The method of the laser pulse self-compression in the process of noise-seeded Raman scattering in a plasma created by a counterpropagating ionized pulse is considered. The sharpness of the ionization front ensures the formation of an output pulse close to the π-pulse solution with a sharp leading edge. The dependence of the gain increment on the transverse wave number leads to the formation of a smooth phase front of the output pulse. The energy efficiency in the output pulse reaches 28% of the total pump energy. A study of the influence of quasistatic inhomogeneities showed only a slight slowdown in the process, even in a plasma with 8% density modulation.

I. INTRODUCTION

Research on amplification and compression of laser pulses in order to achieve extreme values of peak power has been significantly enhanced in the last decade due to the creation of PW laser systems [1,2]. This progress is based on the amplification technique of chirped laser pulses chirped pulse amplification (CPA) and optical parametric CPA (OPCPA). Several projects around the world in the direction of level 10 PW and above are currently underway [3]. The interaction of high-power, high-contrast laser radiation with matter can be used to solve a wide range of fundamental and applied problems. In particular, the creation of compact sources of accelerated proton and ion beams, and the generation of gamma radiation, is a necessary step for high-technology medical applications. High-contrast intense laser pulses can also be used for laboratory modeling of astrophysical processes.

A further increase in the power of the generated laser radiation is associated with significant technical difficulties. This is primarily due to the durability of optical elements with huge laser radiation powers. For example, thermal damage to diffraction gratings occurs with energy fluxes of the order of 0.1 J/cm^2. As a result, for pulses with energies of tens and hundreds of joules, it is necessary to use more and more large-scale meter-sized optical systems, which is technically a very difficult task. Along with this, uniform amplification of laser radiation in a wide frequency range is required, which is also technologically difficult.

To achieve a high power level, it seems natural to use processes in an ionized medium, for which there is no problem of the electric strength of materials. In a transparent plasma, several processes for an intense laser-pulse compression are discussed: (i) the ionization-induced self-compression effect [4,5]; (ii) upon excitation of a wake wave in a plasma [6–11]; (iii) self-compression of laser pulses based on the local nature of relativistic nonlinearity [12–15]; and (iv) as a result of resonant stimulated Raman backscattering (SRBS) [16–18]. The most promising is the latter method for creating a compact ultrapowerful laser system.

Raman amplification is based on resonant three-wave interaction, where a moderately intense and time-extended laser pump pulse at a frequency of ω_a transfers its energy to a short counterpropagating seed laser pulse at a frequency of ω_b through electron plasma oscillations that are excited at the plasma frequency $\omega_p = \omega_a - \omega_b$. When the pump depletion is negligible, the amplitude of the seed laser pulse increases exponentially in time. In this regime, the duration of the amplified pulse increases due to the narrowness of the gain bandwidth of the SRBS process. At the nonlinear stage, when the laser pump pulse is strongly depleted, there is a noticeable increase in the peak intensity at the leading edge of the seed laser pulse, which is much higher than the pump pulse intensity. This increase in intensity accompanies a decrease in the duration of the amplified laser pulse in inverse proportion to the amplitude, which is associated with an increase in the gain bandwidth of the SRBS process with an increase in the amplitude of the amplified laser pulse. The well-known self-similar π-pulse solution is formed [17].

The maximal energy-conversion efficiency is ω_b/ω_a [17]. However, only a weak energetic efficiency (no more than 10%) was demonstrated at the current experimental level [19–24]. This is due to the existence of a number of negative physical processes that can limit the effectiveness of Raman amplification. Most of these negative processes were studied and methods for their neutralization were proposed by choosing the optimal parameters of laser pulses and plasma; in particular, the features of Raman compression under the influence of inhomogeneities of plasma density [25,26], relativistic nonlinearity [27,28], parasitic Raman amplification of plasma noises [17,29,30], the effect of additional plasma ionization [31], damping of pulses due to plasma heating in collisions or through Landau damping [32–34], plasma wave-breaking [17,35,36], and others.

From a practical point of view, the implementation of the SRBS process in plasma seems rather complicated for targeting several powerful laser pulses. Along with the pump and seed pulses, it is desirable to inject an auxiliary wave packet into the gaseous medium to create the plasma of the required density to ensure the condition of three-wave interaction. Moreover, the pulse synchronization should be relatively good (no more than two reverse increments SRBS [37]) if

the pump pulse does not have the required frequency modulation. The creation of a plasma by a pump pulse is not so interesting because, in addition to the possible amplification of plasma noise, it is necessary to use pumping with an intensity above the gas ionization threshold. Obviously, this leads to a decrease in the compression ratio of the pulse since the amplitude of the amplified laser pulse is limited by the influence of relativistic nonlinearity on the three-wave interaction process.

In this paper, we study the possibility of implementing the SRBS process in the absence of a seed laser pulse. In this case, the seed, in fact, is plasma noises. The mechanism of entering the compression mode similar to the π-pulse one is ensured by the absence of amplification before a sharp ionization front counterpropagating to the pump pulse. To achieve favorable conditions for the development of noise amplification in a plasma, a pump without frequency modulation and a plasma density of 10^{19} cm^{-3} and higher were used when the effect of the nonlinear frequency shift of the plasma wave on the Raman amplification process was small [36]. It is shown that the mechanism of the amplified signal clearing from spatial fluctuations is related to the dependence of the decay instability rate on the transverse wave number. On relatively large paths, this ensures the narrow spatial spectrum and, accordingly, the maximal amplification of only "smooth" spatial distributions. Results of three-dimensional numerical simulations are in good agreement with the qualitative model. The study of the influence of weak plasma inhomogeneity on Raman amplification shows that they do not break the self-compression process. The dependence of the linear increment of the Raman instability is obtained, which is in good agreement with the results of numerical simulations.

The paper contents are as follows. Basic equations are formulated in Sec. II. Section III analyzes the SRBS process in the absence of a seed laser pulse. The study of the influence of plasma inhomogeneities on the amplification process is presented in Sec. IV. In the conclusion (Sec. V), the main results of the work are formulated.

II. BASIC EQUATIONS

Let us consider the problem of amplification and compression of circularly polarized laser pulses during stimulated Raman backscattering in a plasma produced by an ionizing pulse during double ionization of molecular hydrogen. Numerical analysis was performed in the framework of three-dimensional equations [36],

$$\partial_t a + \partial_z a - \frac{i}{2}\nabla_\perp^2 a = -bf, \tag{1a}$$

$$\partial_t b - \partial_z b - \frac{i}{2}\nabla_\perp^2 b = af^* + i\beta|b|^2 b, \tag{1b}$$

$$\partial_t f + i\delta\omega(z)f + \nu_f f = ab^* + iB|f|^2 f, \tag{1c}$$

$$\partial_t T_e = \frac{2}{3}\left[\nu_{ei}T_{enl} + 2mc^2\nu_{Lnd}\frac{\omega_a}{\omega_f}|f|^2\right]. \tag{1d}$$

Here, a and b are the amplitudes of the vector potentials of the pump and amplified pulse, respectively, measured in units $mc^2 a_0/e$ ($k_{a,b} = \omega_{a,b}/c$): $A_x + iA_y =$

$\frac{mc^2}{e}a_0(ae^{i\omega_a t - ik_a z} + be^{i\omega_b t + ik_b z})$, where a_0 is the initial amplitude of the pump pulse normalized to the relativistic value. The amplitude of the plasma wave f corresponds to the amplitude of the density perturbation δn_L and the electric floor E_L of the Langmuir wave,

$$E_L = -\frac{mca_0}{e}\sqrt{\frac{2\omega_a}{\omega_f}}\omega_p \, \text{Re}(fe^{i\omega_f t - 2ik_a z}), \tag{2}$$

$$\frac{\delta n_L}{n_0} = -2\sqrt{2}a_0\frac{\omega_a^{3/2}}{\omega_p\omega_f^{1/2}}\text{Im}(fe^{i\omega_f t - 2ik_a z}). \tag{3}$$

The pump frequency ω_a is much larger than the plasma frequency $\omega_p = \sqrt{4\pi n_0 e^2/m}$ and can be considered equal to the frequency of the amplified laser pulse (i.e., $\omega_a \approx \omega_b$); e and m are the charge and mass of the electron, respectively. The frequency $\omega_f = \sqrt{\omega_p^2 + 12\omega_a^2 T_e/mc^2}$ is the frequency of the plasma wave f (which is slightly different from the plasma frequency ω_p due to thermal effects for nonzero electron temperature, $T_e \ll mc^2\omega_p^2/\omega_a^2$). The time t is measured in units of $t_0 = 1/\gamma$ (where $\gamma = a_0\omega_p\sqrt{\omega_a/2\omega_f}$ is the Raman amplification increment), the longitudinal coordinate z is measured in units of ct_0, the transverse coordinate r is measured in units of $c\sqrt{t_0/\omega_a}$, detuning $\delta\omega$ is measured in units of t_0^{-1}, and $\beta = \frac{3\sqrt{2}}{4}a_0\omega_p\omega_f^{1/2}/\omega_a^{3/2}$ is the dimensionless coefficient of relativistic nonlinearity. We neglected the group velocity of the plasma wave, $\frac{\partial\omega_f}{\partial k} = \frac{6T_e}{mc^2}\frac{\omega_a}{\omega_f}$, in Eq. (1c) due to its smallness, $\frac{\partial\omega_f}{\partial k} \ll \gamma\tau_b$, for the parameters considered here, where τ_b is the duration of the seed pulse.

The term $B|f|^2 f$ in Eq. (1c) describes the nonlinear frequency shift (nonlinear dispersion) of the plasma wave f in a rare plasma as its amplitude approaches the rollover threshold [36]. This new term, in comparison with [36], gives the values of Raman amplification, in good agreement with kinetic modeling. Here, $B = 72\sqrt{2}a_0\frac{T_e}{mc^2}\omega_a^{9/2}\omega_f^{1/2}/\omega_p^5$, where T_e is the electron temperature. In particular, Eq. (1d) describes a change in the plasma temperature, where $T_{enl} = mc^2(|a|^2 + |b|^2\frac{\omega_a}{\omega_b} + |f|^2\frac{\omega_a}{\omega_f})$. Electron-ion collision frequency $\nu_{ei} = \frac{2}{3\gamma}\sqrt{\frac{2\pi}{m}}\frac{\Lambda n_e e^4}{T_e^{1/2}(T_e + T_{enl})}$ and the Landau damping rate $\nu_{Lnd} = \frac{\omega_p\sqrt{\pi}}{\gamma(2q_T)^{3/2}}\exp(-\frac{1}{2q_T} - \frac{3}{2})$ for a plasma wave are normalized to the gain ratio γ of backward Raman scattering. Here, $q_T = 4k_a^2 T_e/(\omega_p^2 mc^2)$ is the normalized electron temperature and Λ is the Coulomb logarithm. The initial electron temperature is $T_e \approx 30$ eV, which determines the initial level of δ-correlated noise amplitude for the plasma wave [38],

$$f_{noise} = \sqrt{2\sqrt{2}\pi\frac{a_0 T_e}{mc^2}\sqrt{\frac{\omega_p}{\omega_a}}\frac{t_c\omega_a}{\Delta_r^2\Delta_z}} \simeq 2\times10^{-5}, \tag{4}$$

where $\Delta_r \simeq 0.1$ and $\Delta_z \simeq 0.01$ are dimensionless steps of the computation grid, $t_c = e^2/mc^3$.

III. SPONTANEOUS RAMAN

Let us study the SRBS process in the absence of a seed laser pulse. In this case, the seed, in fact, is plasma noise. The mechanism of entering the compression mode similar to the π-pulse mode is ensured by the absence of amplification in
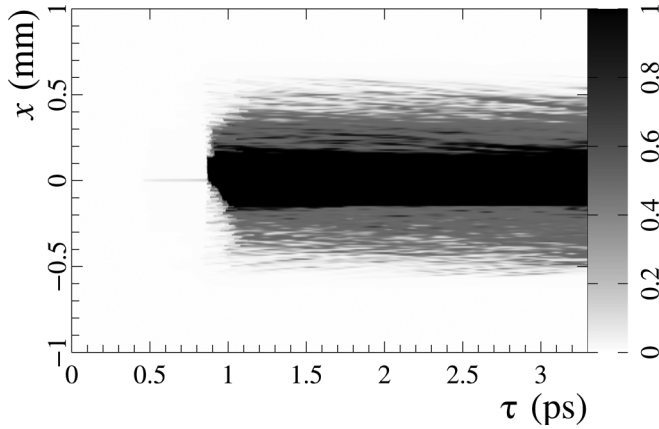
FIG. 1. The typical distribution of the plasma density at the leading edge of the ionization pulse upon double ionization of molecular hydrogen at the 9 mm path which was produced in the process of numerical simulations.

front of a sharp ionization front propagating towards the pump pulse. To achieve favorable conditions for the development of noise amplification in a plasma, it is proposed to use a pump pulse without frequency modulation and a plasma with a concentration of 10^{19} cm^{-3} and higher, in which the influence of the nonlinear dispersion of the plasma wave $B|f|^2$ for the Raman amplification process is not enough [36].

Such a plasma can be created by an ionizing pulse with an intensity of 10^{16} W/cm^2, a duration of 250 fs, and a radius of 300 μm. A typical density profile of the created plasma is shown in Fig. 1. One can see a good uniformity of the generated plasma in the central region.

A. One-dimensional case

Figure 2 shows the one-dimensional dynamics of the SRBS process in the absence of a seed laser pulse in a gas jet
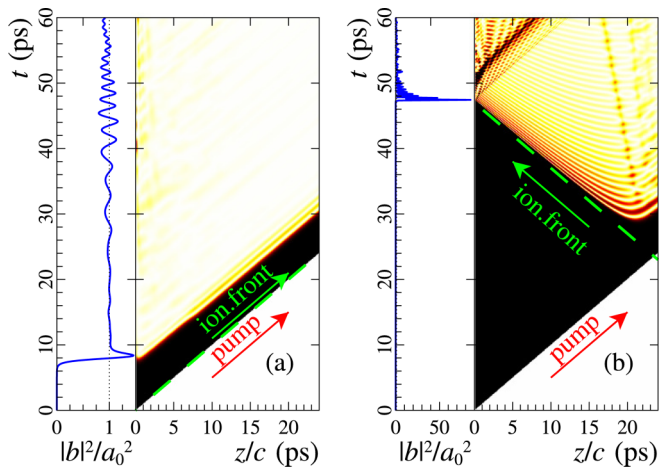

FIG. 2. The one-dimensional dynamics of the SRBS process without a seed laser pulse in a gaseous medium for two cases: (a) pumping and ionizing pulses propagate in the same direction, and (b) pulses propagate towards each other. Plasma length $L = 7.2$ mm, gas density $n_e = 10^{19}$ cm^{-3}, initial plasma noise level 10^{-5}, pump pulse intensity $I_a = 10^{14}$ W/cm^2.

of length $L = 9$ mm, with a gas density of $n_e = 10^{19}$ cm^{-3}; the initial plasma noise level is 10^{-5}, which corresponds to 10^4 W/cm^2 for selected parameters. The calculations were performed for two cases: (a) pumping and ionizing laser pulses propagate in the same direction, and (b) laser pulses propagate towards each other. The pump pulse intensity is $I_a = 10^{14}$ W/cm^2 and the duration is $\tau_a = 60$ ps. This value of the intensity of the pump pulse is not enough for the double ionization of molecular hydrogen. The frequency of the ionizing laser pulse must be outside the three-wave resonance condition,

$$|\omega_a - \omega_{\mathrm{ion}}| \gg \omega_p. \qquad (5)$$

This condition is necessary to exclude the effect of an ionizing pulse on Raman amplification in a plasma.

We turn first to the case of the codirectional propagation of laser pulses [Fig. 2(a)], which are injected from the left side. Pulse propagation directions are indicated by arrows. Obviously, the ionizing pulse is injected a bit earlier than the pump one in order to create a plasma of the required density. The dark region in the figure corresponds to the presence of a pump pulse in a plasma with a maximum amplitude. It can be seen from the figure that the pump pulse penetrates well into the plasma initially. However, amplification of plasma noise reflects a pump pulse with a random phase at $t \gtrsim 7$ ps (approximately $10/\gamma$) with the energy in the reflected wave close to 100% of pump energy. This is clearly seen on the left side of the figure, where the blue curve shows the dependence of the amplitude of the output signal on the left boundary on the time t.

Next, we analyze the case of the counterpropagated laser pulses [Fig. 2(b)]. The pump pulse is injected from the left side, and the ionizing pulse from the right side at the time when the leading edge of the pump pulse reaches it (i.e., at $t = 24$ ps $\approx 50\gamma^{-1}$). Similarly to the case in Fig. 2(a), amplified plasma noises begin to reflect the pump pulse at $t = 24 + 8 = 32$ ps $\approx 65\gamma^{-1}$. Later, the amplified signal continues to propagate in the plasma along with the ionization front and effectively subsequently "eats away" the pump pulse. In the figure, the bright region corresponds to the case when the pump pulse has a small amplitude, and the dark region corresponds to a larger amplitude of the pump. In fact, the initial amplified noise in the plasma acts here as the seed pulse, and the absence of a prepulse is ensured by the absence of three-wave decay before the sharp ionization front. The blue line on the left side of the figure shows the dependence of the amplified laser pulse at the plasma output. It can be seen that the intensity of the output amplified signal exceeded the intensity of the pump pulse by 100 times ($I_b \approx 10^{16}$ W/cm^2), and the pulse duration decreased 1250 times and amounted to $\tau_b \approx 48$ fs. We call this process *self-induced Raman amplification* later.

In Fig. 3, the red line shows the intensity distribution of the amplified pulse. For comparison, the black dotted line shows the π-pulse solution, which corresponds to the ideal case when a seed laser pulse is sent to meet the pump pulse. The duration of the π-pulse solution is 25 fs. A pulse amplified from plasma noises has a duration of approximately two times longer than in the case of a π-pulse solution. This difference
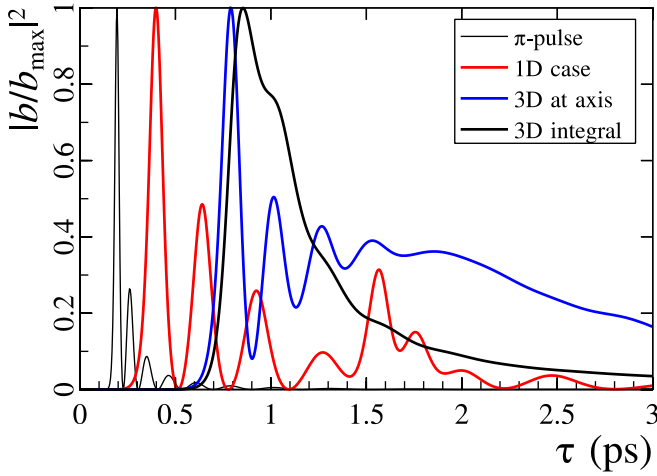
FIG. 3. The time profile of the amplified laser-pulse intensity $|b|^2$ at the output of a jet plasma of 9 mm long with density of $10^{19}\,\mathrm{cm}^{-3}$. The pump intensity is $10^{14}\,\mathrm{W/cm^2}$. The black dotted line shows the π-pulse solution in the one-dimensional case. The red curve shows the amplified pulse in the one-dimensional case. The blue dash-dotted curve shows the amplified pulse in the three-dimensional case on the beam axis. The black curve shows the amplified laser pulse in the three-dimensional case in the focal zone.

is due to decreasing of the actual length of the medium by a quarter over the Raman amplification. This decrease is associated with a buildup of plasma noise to the level of the nonlinear stage of Raman compression. Using a longer plasma allows a greater degree of compression. A few words about energy efficiency. The fraction of energy in the first half-cycle of the π-pulse solution is 89% of the pump energy. In this case of a self-induced Raman amplification, the fraction of energy in the first half-period of the amplified pulse is 61%.

B. Three-dimensional case

The question arises about the structure of the amplified pulse in a non-one-dimensional case. Let us analyze the possibility of realizing a self-induced Raman amplification and compression of a laser pulse in a three-dimensional homogeneous medium. Figure 4 shows the results for such simulation for the plasma length of 9 mm, with density of $n_e = 10^{19}\,\mathrm{cm}^{-3}$. As can be seen from Fig. 1, the uniformity of the produced plasma at scales of 200–300 microns is easily realized. A pump pulse has a duration of 60 ps, transverse size of 100 microns, and intensity of $10^{14}\,\mathrm{W/cm^2}$. Slices of the amplified pulse on the axis of the pump pulse are shown on the rear faces. The lower faces show slices of a focused amplified pulse.
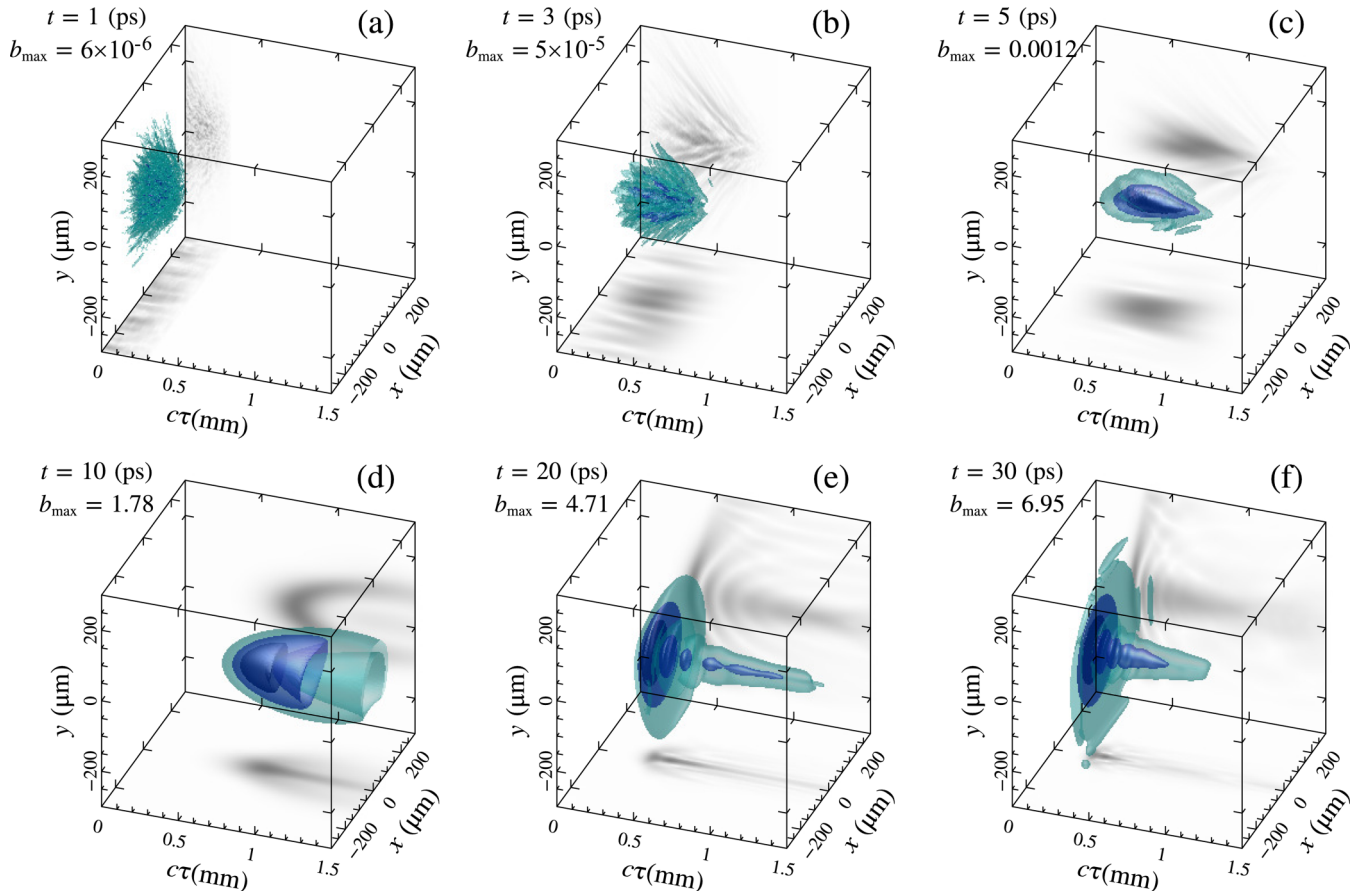

FIG. 4. Three-dimensional dynamics of the SRBS process without a seed laser pulse in the jet plasma at different points in time. The plasma length is $L = 9$ mm, the plasma density is $n_e = 10^{19}\,\mathrm{cm}^{-3}$, the initial plasma noise level is 10^{-5}. Pump pulse intensity $I_a = 10^{14}\,\mathrm{W/cm^2}$, beam radius 100 microns. Rear faces show slices of amplified pulse on the pump axis. Bottom faces show slices of the focused amplified pulse.

It can be seen from the figure that at the initial stage ($t < 9$ ps), the plasma noise is amplified exponentially: the signal amplitude is $b \sim 10^{-5}$ for $t = 1$ ps [Fig. 4(a)] and $b \sim 10^{-4}$ for $t = 3$ ps [Fig. 4(b)]. Along with this, it can be seen from the figure that the amplified noise in the plasma has a wide spatial spectrum (see the lower bound of the figure). As the noise amplitude increases, the amplified noise signal becomes continually smoother in the transverse coordinate [Fig. 4(c)]. Subsequently, an amplified coherent laser pulse is formed from plasma noise. The nonlinear amplification mode is achieved at $t = 9$ ps, when a noticeable depletion of the pump pulse begins. The amplitude of the amplified signal is $b = 1.78$ at time $t = 10$ ps and the spatial spectrum of the signal becomes even narrower (see the lower bound of the figure). Subsequently, a structure similar to the π-pulse solution is formed in the front of the amplified pulse [Figs. 4(e) and 4(f)]. The amplified signal amplitude exceeded the amplitude of the pump pulse by about seven times at the output of the plasma 9 mm long [Fig. 4(f)].

Up to 74% of the pump energy was scattered into the pulse amplified from noise in the process of self-induced Raman amplification. The pump pulse duration decreased from 60 ps to 125 fs in the amplified pulse (the blue dash-dotted line in Fig. 3 shows the profile of the amplified pulse on the beam axis). But the tail of the temporal profile has a rather complex structure in the axial region. However, the spatiotemporal distribution of the amplified pulse has the form of a mushroom [Fig. 4(f)]. Obviously, the fraction of energy in the pulse tail will decrease with a shift from the center of the beam. The black line in Fig. 3 shows the time profile of the amplified pulse in the focal zone. It can be seen that most of the energy is contained in the central part of the pulse. Unfortunately, the pulse duration increased approximately three times. Thus, the results of numerical simulations demonstrate the possibility of shortening the pump pulse from 60 ps to 370 fs with an energy efficiency of 28% of the total pump energy.

It should be noted that the energy efficiency of the process under consideration and the degree of compression are lower than in the case of the π-pulse solution. This is due to the fact that, first, a noticeable part of the medium ($\frac{1}{4} \ldots \frac{1}{3}$ of the entire plasma length) is spent on amplifying plasma noise, which subsequently acts as a seed for a three-wave process. Second, there are significant losses (about half of the energy) associated with cleaning the amplified pulse from the noise signal. The positive side of the process is the narrowing of the spatial spectrum of radiation as it amplifies (see the lower bound in Fig. 4), which makes the output pulse suitable for further focusing.

Let us explain in a simple model the mechanism for cleaning the amplified signal from spatial noise. For this, we analyze the problem of decay of a high-frequency wave a into low-frequency waves b and f in the presence of diffraction effects. After linearizing Eq. (1), assuming the pump field to be unperturbed $a \approx 1$, we obtain equations for small perturbations of the complex envelopes b and f,

$$\partial_t b = f^* - i\nabla_\perp^2 b, \quad \partial_t f = b^*.$$

Substituting a solution of the form $b, f \propto e^{\lambda t - i\vec{k}_\perp \vec{r}}$, we obtain the dispersion relation from the requirement for the existence of a nonzero solution,

$$\det \begin{Vmatrix} \lambda & 0 & 0 & 0 & 0 & 0 \\ 0 & \lambda & 0 & 0 & 0 & 0 \\ 0 & 0 & \lambda - ik_\perp^2 & 1 & 0 & 0 \\ 0 & 0 & 1 & \lambda & 0 & 0 \\ 0 & 0 & 0 & 0 & \lambda + ik_\perp^2 & 1 \\ 0 & 0 & 0 & 0 & 1 & \lambda \end{Vmatrix}$$

$$= \lambda^2[(\lambda^2 - 1)^2 + \lambda^2 k_\perp^4] = 0. \tag{6}$$

This gives an expression for the effective gain ratio,

$$\mathrm{Re}\,\lambda = \sqrt{1 - k_\perp^4/4} \leqslant 1, \tag{7}$$

which is slightly smaller than the one in the ideal case (equal to 1 in dimensionless units). Instability is possible with

$$k_\perp^2 < 2, \tag{8}$$

i.e., pulse diffraction (the term $\nabla_\perp^2 b$) does not stabilize the decay instability but decreases the gain ratio. In dimensional units, the last condition can be rewritten as the smallness of gain length $1/\gamma$ compared to the diffraction length of perturbations with a transverse scale $w \sim 1/k_\perp$.

It follows from expression (7) that the spatial harmonics with $k_\perp \approx 0$ are most effectively amplified. On large paths, this ensures the selection of narrow spectrums in the space of wave vectors and, consequently, the maximum gain of "smooth" spatial distributions. However, the dependence of the increment of decay instability on $k_\perp$ is very smooth for small $k_\perp$. This suggests that the selection by wave vectors will be most effective for narrow wave beams, and may require a significant path for wide beams.

IV. THE EFFECT OF INHOMOGENEITY

Since we plan to use plasma noise as a "seed," the most urgent issue is the possibility of three-wave decay in a weakly inhomogeneous plasma. The reason is that the plasma inhomogeneity introduces an effective detuning of the three-wave resonance, which can stop the Raman amplification. In particular, the use of a plasma density gradient [25] reduces the parasitic amplification of noise in the plasma.

Let us study the decay of a constant high-frequency wave $a = 1$ into low-frequency waves b and f at resonance detuning $\delta\omega$. Linearization of Eq. (1) gives equations for small perturbations of the low-frequency waves b and f,

$$\partial_t b = f^*, \quad \partial_t f + i\delta\omega f = b^*. \tag{9}$$

Substituting a solution of the form $b, f \propto e^{\lambda t}$, we obtain the dispersion relation

$$\lambda^2 + i\delta\omega\,\lambda - 1 = 0, \tag{10}$$

and expression of the gain ratio of Raman instability,

$$\mathrm{Re}\,\lambda = \sqrt{1 - \delta\omega^2/4}. \tag{11}$$

It can be seen from Eq. (11) that the linear stage of Raman scattering is not possible for plasma density fluctuation with the amplitude
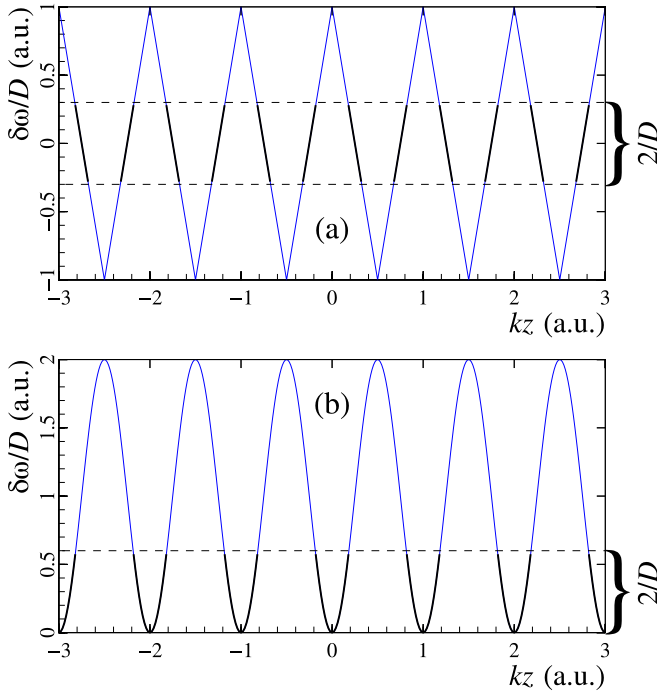
$$|\delta\omega| > 2. \tag{12}$$

FIG. 5. Examples of (a) a sawtooth and (b) a sinusoidal density inhomogeneity. Bold lines indicate the resonance region to estimate the effective gain ratio of the Raman decay.

A similar dependence is usually expected from random quasistatic density fluctuations.

However, plasma fluctuations limited in amplitude do not lead to a breakdown of Raman amplification, but only reduce its rate. Let us dwell on this in more detail. Figure 5 shows two typical examples of plasma density fluctuations: sawtooth [Fig. 5(a)] and sine wave [Fig. 5(b)]. Bold lines indicate multiple regions in the plasma density profile in which the three-wave decay condition $|\delta\omega(z) < 2|$ is satisfied, even for an arbitrarily large fluctuation amplitude of $D = \max \delta\omega$. Linear decay will occur in these areas, but more slowly. Next, we obtain estimates for the expressions of the effective increment of the Raman gain, λ_{eff}, for the two cases under consideration. Remember that $D = \delta\omega$ is the dimensionless quantity, measured in the Raman gain γ.

Obviously, the Raman amplification process is more sensitive to the amplitude of fluctuations in the first case. A rough estimate of the effective increment with a linear change in the density $\delta\omega = kz$ gives an estimate of the effective gain ratio,

$$\lambda_{\text{eff}} \simeq 2 \int \sqrt{1 - (kz)^2} \frac{dz}{L} \approx \frac{\pi}{D}, \qquad (13)$$

where $L = D/k$ is the period of the broken line [Fig. 5(a)]. Thus, the effective increment λ_{eff} decreases inversely with the amplitude of the perturbations. For a similar sinusoidal modulation, $\delta\omega = D \sin(kz)$, the period is longer ($L = \frac{\pi}{2} D/k$), which gives the estimate

$$\lambda_{\text{eff}} = \frac{2}{D}. \qquad (14)$$

However, sinusoidal modulation can provide a significantly greater gain ratio if the center frequency is near the extremes.
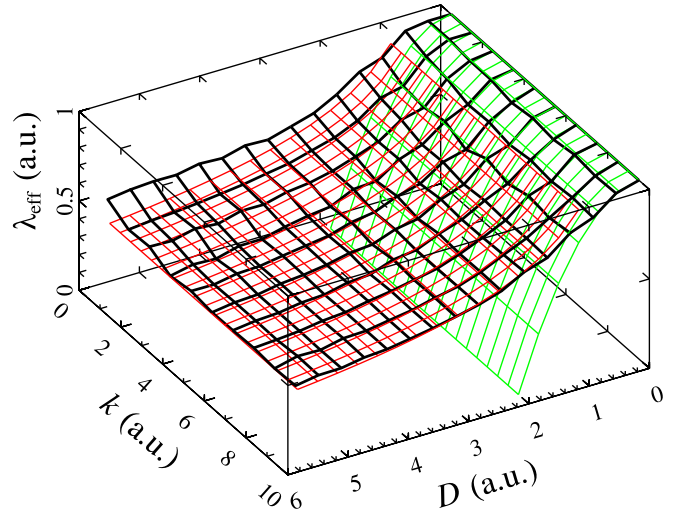

FIG. 6. Dependence of the found numerically effective gain ratio of the Raman amplification in an inhomogeneous plasma $\delta\omega = D \sin(kz)$ on the parameters D and k. Thin red (gray) and green (light gray) grids show analytical estimates (15) and (16).

Then the expansion for large $D \gg 1$ gives the estimate

$$\lambda_{\text{eff}} \simeq \int \sqrt{1 - \frac{D^2(kz)^4}{32}} \frac{dz}{2\pi/k} \approx \frac{0.935}{\sqrt{D}}. \qquad (15)$$

A similar estimate for small $D \ll 1$ is close to the standard one:

$$\lambda_{\text{eff}} \simeq \int \sqrt{1 - D^2 \sin^2(kz)} \frac{dz}{2\pi/k} \approx 1 - \frac{D^2}{4}. \qquad (16)$$

The same estimate is obtained for random inhomogeneities of plasma density.

One-dimensional numerical calculations were performed to verify the found estimate of the effective gain ratio λ_{eff}. A pump pulse with an intensity of 10^{14} W/cm^{-2} was injected into a plasma of $20c/\gamma$ long and density of 10^{19} cm^{-3}. The initial noise level was 10^{-7}. The plasma density fluctuation in the sinelike form of $\delta\omega = D \sin(kz)$ was specified. Such a low noise level was chosen to increase the linear stage of the Raman amplification, when the noise amplitude increases exponentially. Figure 6 shows the numerical dependence of the effective gain ratio on the perturbation amplitude D and k (black lines). Thin red and green grids show analytical estimates (15) and (16), correspondingly. As can be seen from the figure, a qualitative assessment of the effective increment is in good agreement with the results of numerical simulation.

Thus, fluctuations of plasma density limited in amplitude do not lead to breaking of the proposed compression method, but only increase the length of reaching the nonlinear mode. Indeed, one can expect that the effective gain increment for large fluctuations of $D \gg 1$ lies in the range given by Eqs. (14) and (15),

$$\frac{2}{D} \lesssim \lambda_{\text{eff}} \lesssim \frac{1}{\sqrt{D}}. \qquad (17)$$

Next, we turn to the structure of the amplified pulse in the three-dimensional problem. Figure 7 shows the spatiotemporal dynamics of a pulse in a plasma that is 9 mm long with
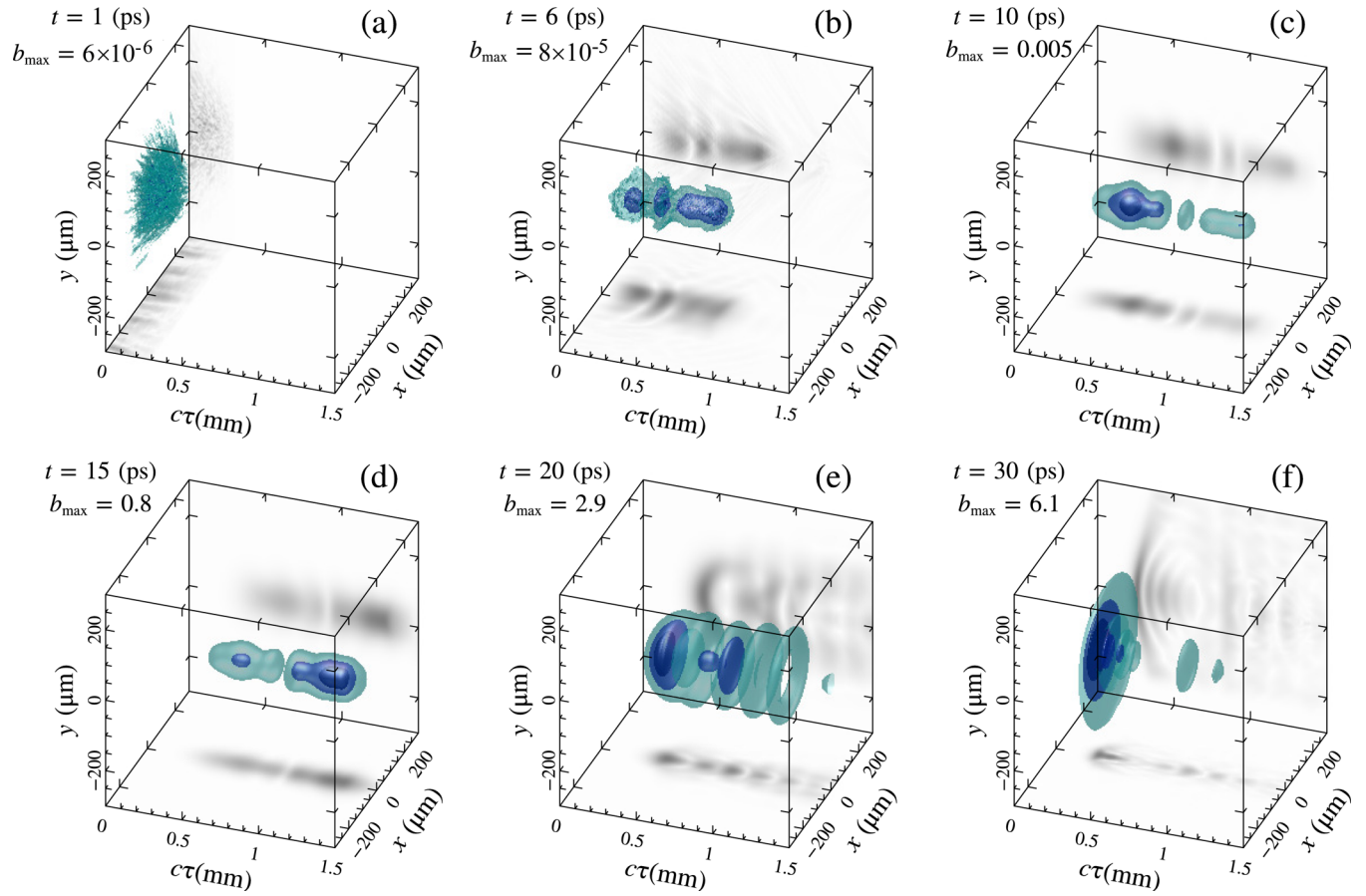
FIG. 7. Similar to Fig. 4, but for the plasma inhomogeneity $\delta\omega = D\sin(\gamma z/c)$ with $D = 6$, corresponding to a 8% fluctuation of the plasma density.

a concentration of 10^{19} cm^{-3}. In the medium, plasma density fluctuations are of the form $\delta\omega = 6\sin(z)$. This corresponds to a 8% fluctuation in plasma density. It can be seen from the figure that the self-induced Raman amplification in this case continues almost as in homogeneous media. Moreover, the depth of plasma density fluctuations D is three times higher than the classical threshold (12) at which the three-wave process should not have occurred. As can be seen from the figure, the self-induced Raman amplification at these parameters proceeds slightly slower than in a homogeneous medium (see Fig. 4), since the effective increment in this case is approximately 1.7 times smaller than the increment for a homogeneous medium.

V. CONCLUSION

The paper is devoted to the self-compression mode of a laser pulse in the process of spontaneous Raman scattering in the absence of a seed pulse in a plasma produced by a counterpropagating ionized pulse. The mechanism for the amplified noise signal to enter a compression mode similar to a π-pulse mode is ensured by the absence of amplification in front of a sharp ionization front. To achieve favorable conditions for the development of noise amplification in a plasma, a pump without frequency modulation and a plasma with a density of 10^{19} cm^{-3} and higher were used when the

effect of the nonlinear frequency shift of the plasma wave on the Raman amplification process was small.

The dependence of the decay instability coefficient on the transverse wave number leads to amplification of only a narrow spectrum of wave vectors. On relatively large paths, this ensures maximum amplification of "smooth" spatial distributions. As a result, the phase front of the amplified signal becomes almost uniform, and the output pulse itself is well focused. The results of three-dimensional numerical modeling are in good agreement with the qualitative model. In this case, the energy efficiency in the forward pulse reaches 28% of the total pump energy. However, this method greatly simplifies the beam targeting scheme, which is especially important when using high-power laser pulses.

A study of the influence of quasistatic density inhomogeneities showed the absence of amplification breaking even in a highly inhomogeneous plasma with 10–20% density modulation. The dependence of the linear increment of the Raman instability is obtained, which is in good agreement with the results of three-dimensional calculations. For example, in 8% of the nonuniformity of the plasma density, only a slight slowdown of the amplification process in the plasma occurs.

[1] J. H. Sung, H. W. Lee, J. Y. Yoo, J. W. Yoon, C. W. Lee, J. M. Yang, Y. J. Son, Y. H. Jang, S. Ku Lee, and C. H. Nam, Opt. Lett. **42**, 2058 (2017).

[2] X. Zeng, K. Zhou, Y. Zuo, Q. Zhu, J. Su, X. Wang, Xi. Wang, X. Huang, X. Jiang, D. Jiang, Y. Guo, N. Xie, S. Zhou, Z. Wu, J. Mu, H. Peng, and F. Jing, Opt. Lett. **42**, 2014 (2017).

[3] https://eli-laser.eu/the-eli-project/; http://www.izest.polytechnique.edu/.

[4] S. A. Skobelev, A. V. Kim, and O. Willi, Phys. Rev. Lett. **108**, 123904 (2012).

[5] N. L. Wagner, E. A. Gibson, T. Popmintchev, I. P. Christov, M. M. Murnane, and H. C. Kapteyn, Phys. Rev. Lett. **93**, 173902 (2004).

[6] A. Pipahl, E. A. Anashkina, M. Toncian, T. Toncian, S. A. Skobelev, A. V. Bashinov, A. A. Gonoskov, O. Willi, and A. V. Kim, Phys. Rev. E **87**, 033104 (2013).

[7] A. A. Balakin, A. G. Litvak, V. A. Mironov, and S. A. Skobelev, Phys. Rev. A **88**, 023836 (2013).

[8] A. V. Kim, A. G. Litvak, V. A. Mironov, and S. A. Skobelev, Phys. Rev. A **90**, 043843 (2014).

[9] A. A. Balakin, A. G. Litvak, V. A. Mironov, and S. A. Skobelev, Europhys. Lett. **100**, 34002 (2012).

[10] J. Faure, Y. Glinec, J. J. Santos, F. Ewald, J.-P. Rousseau, S. Kiselev, A. Pukhov, T. Hosokai, and V. Malka, Phys. Rev. Lett. **95**, 205003 (2005).

[11] J. Schreiber, C. Bellei, S. P. D. Mangles, C. Kamperidis, S. Kneip, S. R. Nagel, C. A. J. Palmer, P. P. Rajeev, M. J. V. Streeter, and Z. Najmudin, Phys. Rev. Lett. **105**, 235003 (2010).

[12] O. Shorokhov, A. Pukhov, and I. Kostyukov, Phys. Rev. Lett. **91**, 265002 (2003).

[13] C. Ren, B. J. Duda, R. G. Hemker, W. B. Mori, T. Katsouleas, T. M. Antonsen, Jr., and P. Mora, Phys. Rev. E **63**, 026411 (2001).

[14] A. Sharma and I. Kourakis, Plasma Phys. Control. Fusion **52**, 065002 (2010).

[15] T. C. Wilson, F. Y. Li, S. M. Weng, M. Chen, P. McKenna, and Z. M. Sheng, J. Phys. B **52**, 055403 (2019).

[16] V. M. Malkin, G. Shvets, and N. J. Fisch, Phys. Rev. Lett. **82**, 4448 (1999).

[17] V. M. Malkin, G. Shvets, and N. J. Fisch, Phys. Plasmas **7**, 2232 (2000).

[18] J. Ren, W. Cheng, S. Li, and S. Suckewer, Nat. Phys. **3**, 732 (2007).

[19] Y. Ping, W. Cheng, S. Suckewer, D. S. Clark, and N. J. Fisch, Phys. Rev. Lett. **92**, 175007 (2004).

[20] A. A. Balakin, D. V. Kartashov, A. M. Kiselev, S. A. Skobelev, A. N. Stepanov, and G. M. Fraiman, JETP Lett. **80**, 12 (2004).

[21] Y. Ping, I. Geltner, and S. Suckewer, Phys. Rev. E **67**, 016401 (2003).

[22] X. Yang, G. Vieux, E. Brunetti, B. Ersfeld, J. P. Farmer, M. S. Hur, R. C. Issac, G. Raj, S. M. Wiggins, G. H. Welsh, S. R. Yoffe, and D. A. Jaroszynski, Sci. Rep. **5**, 13333 (2015).

[23] G. Vieux, A. Lyachev, X. Yang, B. Ersfeld, J. P. Farmer, E. Brunetti, R. C. Issac, G. Raj, G. H. Welsh, S. M. Wiggins, and D. A. Jaroszynski, New J. Phys. **13**, 063042 (2011).

[24] G. Vieux, S. Cipiccia, and D. A. Jaroszynski, Sci. Rep. **7**, 2399 (2017).

[25] A. A. Solodov, V. M. Malkin, and N. J. Fisch, Phys. Plasmas **10**, 2540 (2003).

[26] A. A. Balakin, I. Y. Dodin, G. M. Fraiman, and N. J. Fisch, Phys. Plasmas **23**, 083115 (2016).

[27] V. M. Malkin, Z. Toroker, and N. J. Fisch, Phys. Rev. E **90**, 063110 (2014).

[28] I. Barth, Z. Toroker, A. A. Balakin, and N. J. Fisch, Phys. Rev. E **93**, 063210 (2016).

[29] V. M. Malkin, G. Shvets, and N. J. Fisch, Phys. Rev. Lett. **84**, 1208 (2000).

[30] A. A. Balakin, G. M. Fraiman, N. J. Fisch, and V. M. Malkin, Plasma Phys. **10**, 4856 (2003).

[31] A. A. Balakin, G. M. Fraiman, N. J. Fisch, and S. Suckewer, Phys. Rev. E **72**, 036401 (2005).

[32] V. M. Malkin, N. J. Fisch, and J. S. Wurtele, Phys. Rev. E **75**, 026404 (2007).

[33] A. A. Balakin, N. J. Fisch, G. M. Fraiman, V. M. Malkin, and Z. Toroker, Phys. Plasmas **18**, 102311 (2011).

[34] S. Depierreux, V. Yahia, C. Goyon, G. Loisel, P.-E. Masson-Laborde, N. Borisenko, A. Orekhov, O. Rosmej, T. Rienecker, and C. Labaune, Nat. Commun. **5**, 4158 (2014).

[35] R. M. G. M. Trines, F. Fiuza, R. Bingham, R. A. Fonseca, L. O. Silva, R. A. Cairns, and P. A. Norreys, Nat. Phys. **7**, 87 (2011).

[36] A. A. Balakin, G. M. Fraiman, Q. Jia, and N. J. Fisch, Phys. Plasmas **25**, 063106 (2018).

[37] A. A. Balakin, G. M. Fraiman, D. S. Levin, and S. A. Skobelev, Phys. Plasmas **27**, 053106 (2020).

[38] Ph. Mounaix, D. Pesme, W. Rozmus, and M. Casanova, Phys. Fluids B **5**, 3304 (1993).